EPJ manuscript No.
(will be inserted by the editor)

Proton Branching Ratios in ^{22}Mg for X-ray Bursts

S. H. Kim[1], K. Y. Chae[1a], D. W. Bardayan[2], J. C. Blackmon[3,4], K. A. Chipps[4,5,6], R. Hatarik[7,8], K. L. Jones[6], M. J. Kim[1], R. L. Kozub[9], J. F. Liang[4], C. Matei[10,11], B. H. Moazen[6], C. D. Nesaraja[4,6], P. D. O'Malley[2,12], S. D. Pain[4,8], and M. S. Smith[4]

[1] Department of Physics, Sungkyunkwan University, Suwon 16419, Republic of Korea

[2] Department of Physics, University of Notre Dame, Notre Dame, Indiana 46556, USA

[3] Department of Physics and Astronomy, Louisiana State University, Baton Rouge, Louisiana 70803, USA

[4] Physics Division, Oak Ridge National Laboratory, Oak Ridge, Tennessee 37831, USA

[5] Colorado School of Mines, Golden, Colorado 80401, USA

[6] Department of Physics and Astronomy, University of Tennessee, Knoxville, Tennessee 37996, USA

[7] Lawrence Livermore National Laboratory, Livermore, California 94550, USA

[8] Department of Physics and Astronomy, Rutgers University, Piscataway, New Jersey 08854, USA

[9] Department of Physics, Tennessee Technological University, Cookeville, Tennessee 38505, USA

[10] Extreme Light Infrastructure–Nuclear Physics (ELI-NP), Horia Hulubei National Institute for R&D in Physics and Nuclear Engineering (IFIN-HH) 077125 Buchurest-Magurele, Romania

[11] Oak Ridge Associated Univesities, Oak Ridge, Tennesse 37831, USA

[12] Department of Physics and Astronomy, Rutgers University, New Brunswick, New Jersey 08903, USA

Received: date / Revised version: date

Abstract. Decay protons from ^{22}Mg energy levels populated through a previously reported ^{24}Mg(p, t)^{22}Mg transfer reaction [Chae *et al.*, Phys. Rev. C **79**, 055804 (2009)] have been analyzed for proton branching ratios as a follow-up analysis. The measurement was performed at the Holifield Radioactive Ion Beam Facility of Oak Ridge National Laboratory by utilizing 41-MeV proton beams and ^{24}Mg solid targets. Decay protons and reaction tritons were simultaneously detected with a silicon detector array. By investigating the ^{24}Mg(p, t)^{22}Mg*(p)^{21}Na channels, the proton branching ratios of five ^{22}Mg excited states were obtained. The measured branching ratios provide constraints on the proton partial widths of the populated ^{22}Mg levels, which have implications for X-ray burst nucleosynthesis.

1 Introduction

X-ray bursts (XRB) are some of the most interesting astrophysical phenomena, and occur in the atmosphere of an accreting neutron star in close binary star systems. [1] Heavy elements up to Cd-Sn can be synthesized during the burst within ∼10 seconds through thermonuclear reactions on proton-rich unstable nuclei. Since thermonuclear reactions power XRBs, many nuclear parameters should be well studied to understand XRB properties such as peak temperatures, luminosity, and isotopic abundances produced via nucleosynthesis. It is believed that the breakout from the hot CNO cycle can be provided through the ^{18}Ne(α, p)^{21}Na reaction when the critical values of density and temperature are reached [2]. Then the ^{21}Na(p, γ)^{22}Mg reaction can initiate the rapid proton capture process (rp-process) [3,4].

Despite its importance, the ^{21}Na(p, γ)^{22}Mg reaction rate at typical XRB temperatures is still controversial. The reaction rates reported by Cyburt *et al.* [5] and that by Iliadis *et al.* [6] differ by one order of magnitude. Cyburt *et al.* calculated the ^{21}Na(p, γ)^{22}Mg reaction rate theoretically using the NON-SMOKER^{WEB} code version 5.0w [7]. Iliadis *et al.* obtained the ^{21}Na(p, γ)^{22}Mg reaction rate using a Monte-Carlo method with empirical resonance parameters mainly adopted from Ref. [8] and [9]. Therefore, more measurements are needed to better estimate the reaction rate at XRB temperatures.

Since the ^{21}Na(p, γ)^{22}Mg reaction rate strongly depends on the properties of ^{22}Mg energy levels above the proton threshold at 5.504 MeV, many resonance parameters including the excitation energies, spins, parities and partial widths of the levels are required to estimate the reaction rate correctly. Although many parameters have been revealed through previous studies utilizing various nuclear reactions [8–17], there are still remaining parameters yet to be determined.

The ^{24}Mg(p, t)^{22}Mg transfer reaction was previously studied to clarify the level structure of ^{22}Mg especially above the α-threshold at 8.14 MeV [15], which enabled the astrophysical ^{18}Ne(α, p)^{21}Na reaction rate to be updated accordingly. The angular distributions of the reaction tritons were extracted for seven ^{22}Mg energy levels. The empirical angular distributions were then compared with the Distorted Wave Born Approximation (DWBA) calculations to deduce the spins and parities of the energy levels by using computer code DWUCK5 [18]. In the present work, the proton decay channels of several ^{22}Mg levels populated from the ^{24}Mg(p, t)^{22}Mg reaction are investigated as a follow-up analysis.

The experiment was performed at the Holifield Radioactive Ion Beam Facility (HRIBF) at Oak Ridge National Laboratory (ORNL) [19] using 41 MeV proton beams and ^{24}Mg foils. The thickness of isotopically-enriched (>99.9%) ^{24}Mg target was approximately 500 μg/cm^2. The beam current was continuously monitored with a graphite beam stop located downstream of the target chamber. The recoiling particles were detected by the annular silicon detector array, SIDAR [20]. The SIDAR was composed of three trapezoidal wedges of 100-μm-thick $\triangle$E and 1000-

[a] e-mail: kchae@skku.edu

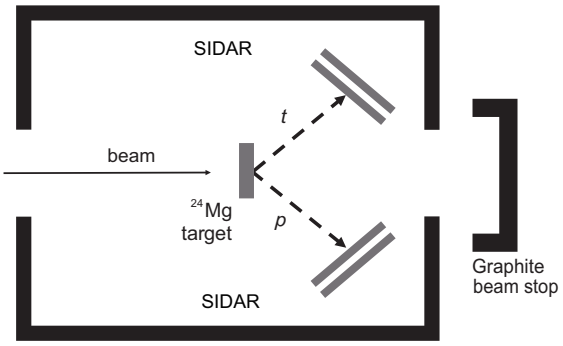

Fig. 1. A schematic diagram of the experimental setup.

μm-thick E telescopes. Each detector was segmented into 16 strips. The light recoil particles were identified by standard energy loss techniques. As shown in Fig. 2 of Ref. [15], the tritons from the ^{24}Mg(p, t)^{22}Mg reaction were clearly identified without significant contamination from other charged particles. The SIDAR covered the angular range of 18°$\leq \theta_{lab} \leq$48°. The energy gain of each strip was calibrated using 5.8-MeV α particles from a ^{244}Cm radioactive source. The triton energies were then internally calibrated by using the well-known ^{22}Mg levels at E_x = 1.247, 3.308, 4.402, and 6.045 MeV. A schematic diagram of the experimental setup is shown in Fig. 1.

2 Analysis

2.1 Coincidence between reaction tritons and decay protons

As demonstrated previously [21,22,24], proton branching ratios can be extracted serendipitously from existing reaction data by comparing the number of times a resonance was formed, via the reaction products, with the number of times it decayed, via coincident decay particles. In this analysis, the number of the tritons from the

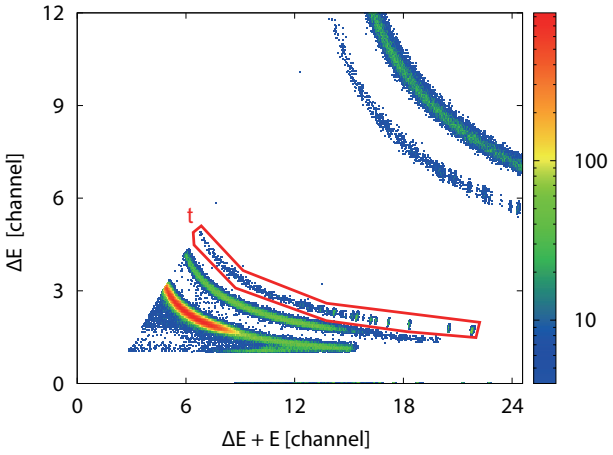

Fig. 2. Particle identification plot obtained at $\theta_{lab} = 37°$. The red solid line is a gate for identifying the reaction tritons.

^{24}Mg(p, t)^{22}Mg reaction and that of the decay protons were needed. A typical PID plot obtained at $\theta_{lab} = 37°$ is shown in Fig. 2. The events falling in the red gate are identified as tritons. Only the low-energy protons (0.8 MeV < E_p < 3.2 MeV) stopped in the ΔE detectors were analyzed for the present work, because the experimental setup such as the proton beam energy, detector thickness and detector threshold was optimized for the ^{24}Mg(p, t)^{22}Mg transfer reaction study.

By requiring a coincidence between the reaction tritons and the decay protons in the time window of 40 ns, the events from the proton decay of ^{22}Mg energy levels could be identified as shown in Fig. 3, which shows the two dimensional spectrum of proton energy (E_p) versus triton energy (E_t). Two diagonal bands in the figure represent the events associated with ^{24}Mg(p, t)^{22}Mg*(p)^{21}Na channels. The upper gate, labeled as p0, shows the decay events from the excited states of ^{22}Mg to the ground state of ^{21}Na. Similarly, the events in the p1 gate are correlated

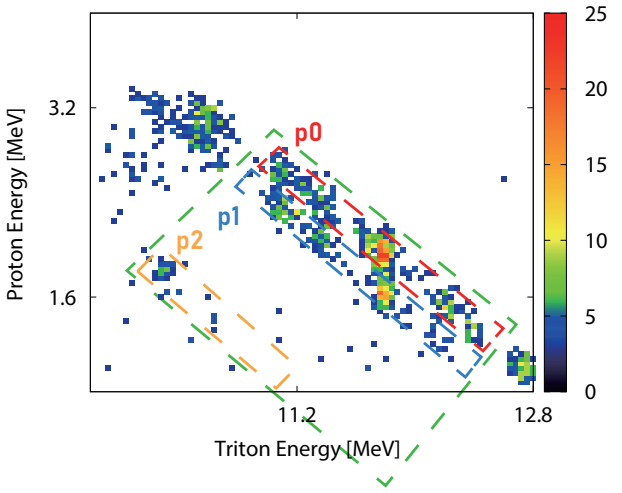

Fig. 3. Two-dimensional energy spectrum of the coincident proton energy (E_p) versus triton energy (E_t). Diagonal gates labeled as p0 and p1 are drawn to analyze the corresponding decay channel. The p2 gate is also drawn but not analyzed because of insufficient statistics. The green gate is for constructing the ^{21}Na excitation energy spectrum (See text).

to the decays to the first excited state of ^{21}Na ($E_x = 0.332$ MeV). The events appearing at right-bottom side, $E_t >$ 12.3 MeV, seem to have clear structure in Fig. 3 and Fig. 5. However, they were not analyzed, since the discriminator threshold of several silicon strip detectors were rather high and therefore the protons at the energies relevant for the group were not recorded. The clusters at left-bottom side in the figure were identified as the decay events to the second excited state of ^{21}Na ($E_x = 1.716$ MeV) by constructing the ^{21}Na excitation energy spectrum (Fig. 4). However, they were also excluded in the present analysis because of insufficient statistics.

To see if the coincident events do originate from the proton decay of ^{22}Mg levels, the high energy protons ($E_p >$ 3.2 MeV) that can be clearly identified from the particle identification plot were considered. Using the protons, the coincident events were plotted in similar way. The result shows that the diagonal bands in Fig. 3 are well extrapolated from those obtained using the high energy protons. Kinematics calculations show that other decay channels such as ^{24}Mg(p, t)^{22}Mg*(d)^{20}Na are not possible.

Due to the rather small excitation energy of the first excited state, two groups in the figure are not well separated. To estimate the uncertainty caused from this issue, the ^{21}Na excitation energy spectrum was constructed. A large gate that includes the p0 and p1 gates was drawn as shown in Fig. 3 (green dashed line). Based on the relativistic 4-vector kinematics considerations of the particles participating in the reaction such as protons, tritons, ^{24}Mg, ^{22}Mg, and ^{21}Na ions, the coincident events were projected into the ^{21}Na excitation energy. For each event in the gate, the excitation energy of ^{22}Mg, E_{22mg}, can be obtained using

$$\begin{aligned}(E_{22mg} + m_{22mg})^2 = {} & m_p{}^2 + m_{24mg}{}^2 + m_t{}^2 \\ & - 2(m_p + T_p)(m_t + T_t) \\ & + 2(m_p + T_p)m_{24mg} - 2(m_t + T_t)m_{24mg} \\ & + \sqrt{[(m_p + T_p)^2 - m_p{}^2][(m_t + T_t)^2 - m_t{}^2]}\ \cos\theta,\end{aligned} \quad (1)$$

where T and m are the kinetic energy measured in the laboratory frame (in MeV) and the mass (in MeV/c^2) of the corresponding particle, respectively. The excitation energy of ^{21}Na, E_{21Na}, is then expressed as

$$E_{21na} = E_{22mg} + m_{22mg} - T_p - m_p - m_{21na}. \quad (2)$$

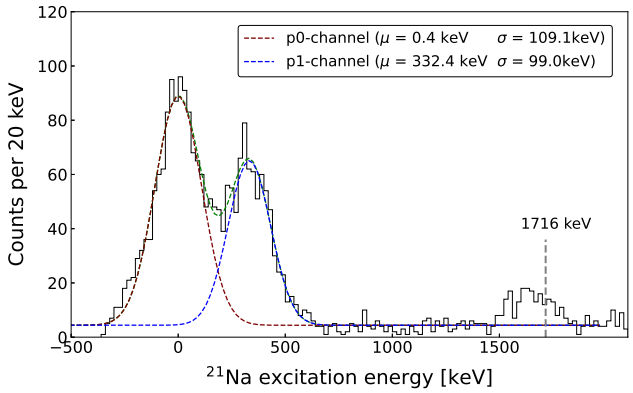

Fig. 4. The reconstructed ^{21}Na excitation energy spectrum from the decay events in the green gate shown in the Fig. 3. The values of the centroids μ and standard deviations σ are presented on the figure. The standard error means are 3.4 keV and 3.7 keV for the centroids of p0 and p1 channels, respectively. The peak near E_x = 1.716 MeV is from the decay events in the p2 gate of Fig. 3.

Using the equations above, the ^{21}Na excitation energy spectrum could be constructed as shown in the Fig. 4. The events were well fitted by Gaussian distributions. The difference between the values of the centroids was 0.333 ± 0.007 MeV, which agreed well with the energy difference between the ground state and the first excited state of ^{21}Na. Additionally, the decay events appearing at the left bottom side on the Fig. 3 are also plotted in the figure. The result shows that the reconstructed energies of the events appear near E_x = 1.716 MeV, which is the excitation energy of the second excited state of ^{21}Na. Therefore, it can be concluded that the events originated from the p2 channel. The uncertainties of the branching ratios caused by overlapping events were estimated to be about 5.0% for the p0 channel and 7.6% for the p1 channel.

The triton energy spectra were reconstructed next as shown in Fig. 5. The red dashed line and blue dotted line represent the spectrum obtained from the p0-gated and p1-gated events, respectively. The black solid line is the triton single energy spectrum adopted from the ^{24}Mg(p, t)^{22}Mg study [15]. A total of 8 excited states in ^{22}Mg were identified above the proton-threshold with enough statistics.

The extracted values of excitation energies were internally calibrated using three well-known reference points: the energy levels at E_x = 6.043 MeV, 7.218 MeV, and 7.967 MeV. Not all identified levels were analyzed in the present work. For instance, the 7.967 MeV and 7.356 MeV states are not considered, as they are suspected doublets [14,17]. Five excited states studied in the present work (E_x = 6.766, 6.876, 7.218, 7.599 and 7.810 MeV) and three reference points are labeled with their excitation energies in the figure.

Each spectrum in Fig. 5 was fitted assuming Gaussian distributions for populated levels with a constant background term. The peaks in the triton single spectrum were fitted first. Then, the corresponding peaks in the proton gated spectrum were fitted, using the same values of centroids and widths. The width of the peaks were fixed to be 40 keV for all considered peaks. From the fitting result, the background was estimated to be about 75 counts per 5 keV for triton single spectrum and 2 counts per 5 keV for proton gated spectra. One example for the E_x = 7.599MeV level is shown in Fig. 6. Fig. 6 (a), (b), and (c)

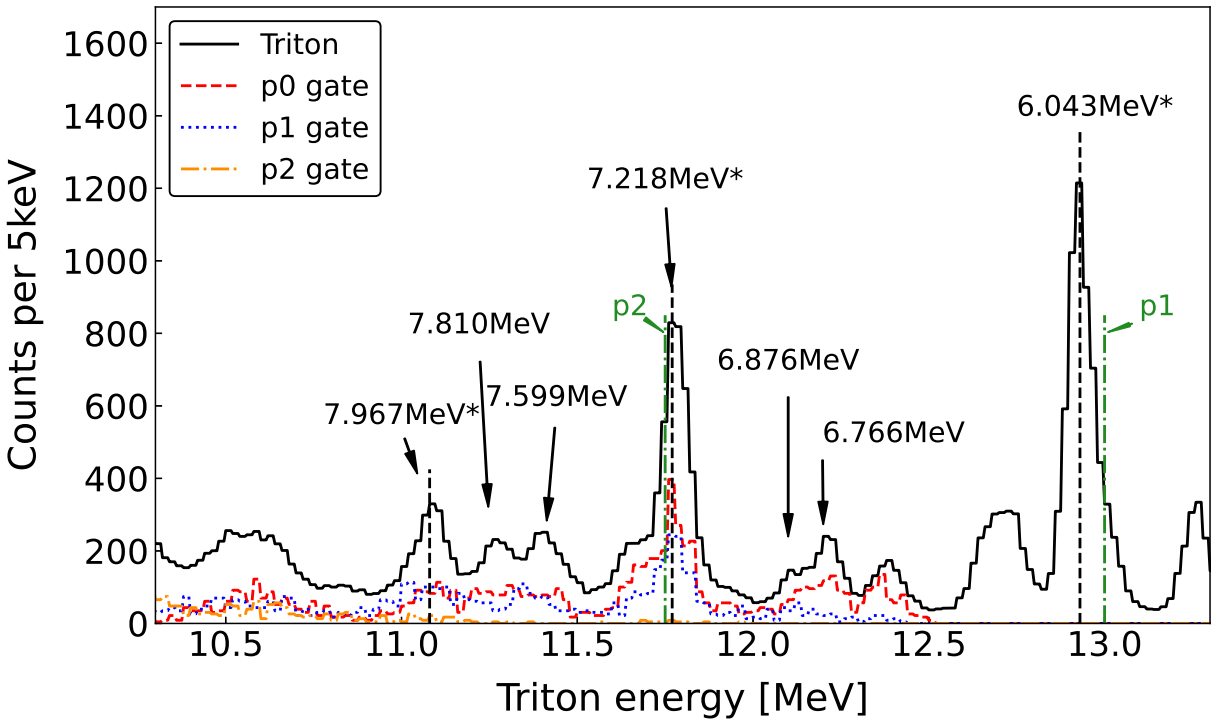

Fig. 5. The triton energy spectrum obtained at $\theta_{lab} = 33^{\circ}$ is shown as a black solid line, which is adopted from Ref. [15]. The identified levels and reference points are labeled with their excitation energies. The reference points are marked with an asterisk. The dashed vertical black lines represent the reference points used for the energy calibration. The spectra from the p0, p1 and p2 gate are corrected by the detection efficiency. The two vertical green lines represent the p1 and p2-threshold.

show the results of the fittings for the triton single, p0 gated and p1 gated triton energy spectra, respectively.

By integrating each Gaussian function using fine tuned fitting parameters from (centroid)-(3σ) to (centroid)+(3σ), about 99.7% of the tritons and coincident protons could be reliably counted. From the ratio of the number of protons and that of tritons, the proton branching ratio of the ^{22}Mg excited state could be calculated. Because the solid angle covered by SIDAR was only about 6% of 4π and therefore not all protons from the decay of ^{22}Mg levels were detected, the total number of decay protons had to be corrected for the geometric detection efficiency. The solid angle covered by each strip of the SIDAR was obtained using a calibrated alpha emitting source, ^{244}Cm. The measured solid angle values agreed with geometric calculations within 3%. The result is summarized in Table 1.

2.2 Isotropic assumption

The branching ratio calculation in the previous section procedure described above is valid when the decay of protons is isotropic. To verify the validity of this assumption,

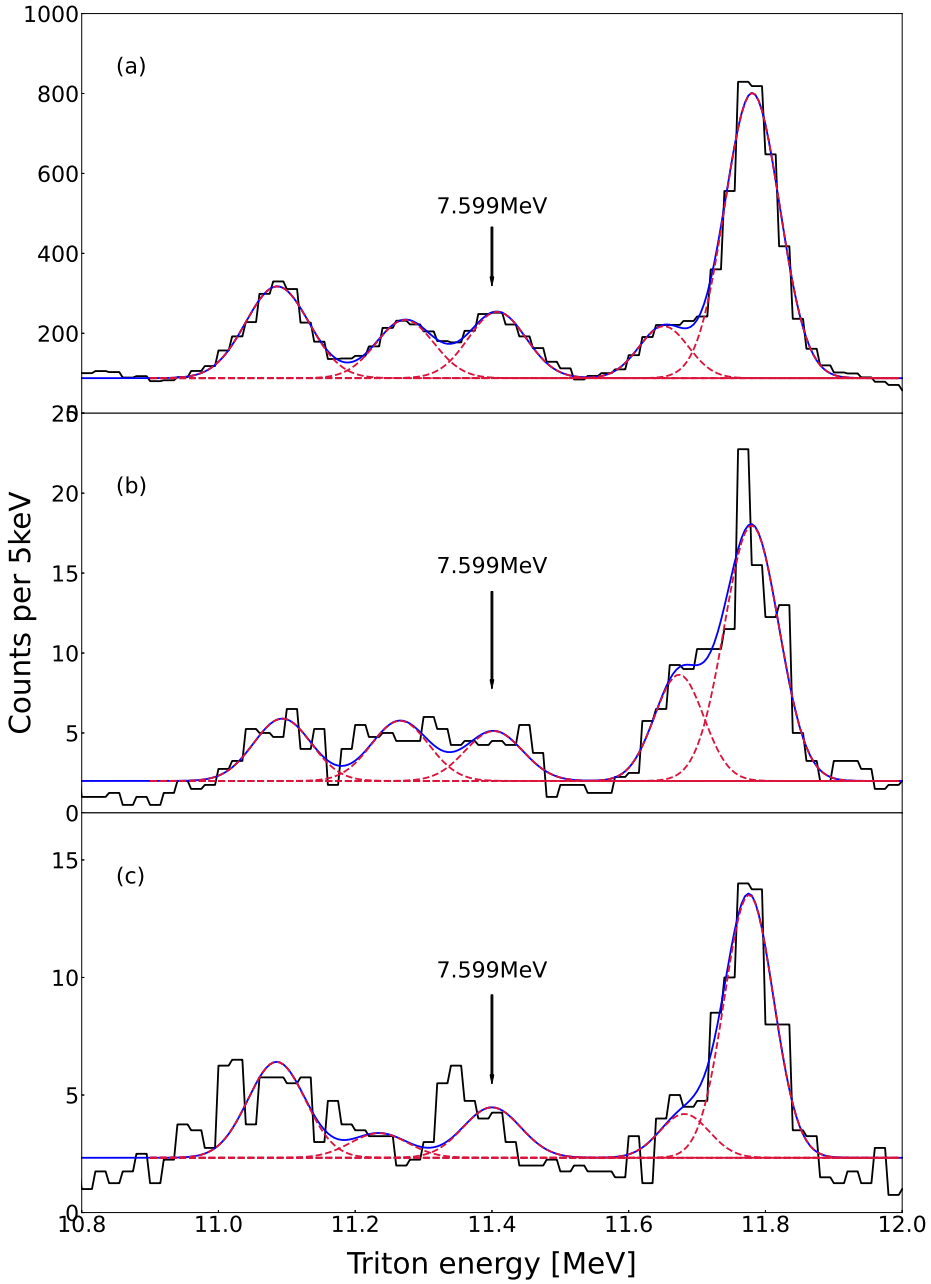

Fig. 6. The fitted energy spectra of (a) triton single, (b) p0- and (c) p1-gated events for the E_x = 7.599 MeV level. The blue solid line is the sum of the constant term and the Gaussian distributions which are shown as the red dashed lines.

Table 1. The results of the branching ratio calculations. The excitation energies are taken from Ref. [23]. The value of B_{p1} is not computed for the states at E_x = 6.766 and 6.876 MeV because of the poor statistics in the p1-gated spectrum. The branching ratios are calculated assuming the isotropic decay of protons (See text). The total uncertainty includes the isotropic uncertainty and statistical uncertainty.

	E_x [MeV] [23]	B_{p0}	B_{p1}
Sp_1 = 5.831	6.766±0.012	0.54±0.18	
	6.876±0.012	0.81±0.30	
	7.218±0.001	0.38±0.12	0.24±0.08
Sp_2 = 7.220	7.599±0.003	0.33±0.12	0.23±0.10
	7.810±0.040	0.45±0.16	0.13±0.08

a simple test was implemented. For each identified decay proton, the angle between a triton and the coincident proton pair measured in the laboratory frame, θ_{lab}, was calculated by considering the geometry of SIDAR described in section 1. The histograms of relative angles for the decay events from the 7.218 MeV state of ^{22}Mg to the ground and first excited state of ^{21}Na are shown as the black solid lines in Fig. 7. The statistical uncertainties are indicated as the error bars.

The experimental distribution was then compared with theoretical calculations. Calculated relative angle histograms obtained from the isotropic decay of protons in the center of mass frame are shown as blue-dashed lines. As shown in the figure, the isotropic decay lines well reproduce the experimental data regardless of the value of transferred angular momentum. Relative angle histograms for anisotropic decay are also shown in the figure as red-dotted lines. Unlike the previous proton branching ratio studies which used randomly biased cosine variations for anisotropic decay calculations [26–28], the calculated proton distributions were biased using the Legendre polynomials with proper angular transfer values in the present work. For instance, for the transition from the 7.218 MeV state ($J^\pi = 0^+$) to the ground state ($J^\pi = 3/2^+$), the Legendre Polynomial with $l = 2$ $P_{l=2}(cos\theta)$ was assumed.

It is obvious from the figure that the isotropic decay assumption better reproduces the experimental result. Therefore, it is concluded that the proton decays are largely isotropic even when transferred angular momentum l is not 0. This conclusion is consistent with those from Refs. [26–28]. In order to account for any discrepancies between the anisotropic and isotropic decay, the systematic uncertainty is introduced, as previously done in Refs. [24–28]. In Ref. [24], for instance, the angular correlations between the heavy recoils and decay particles were calculated for proton decays with l = 0 to 3. The result shows that the uncertainties caused by the anisotropic decay assumption are from 5% to 30% depending on the value of l = 1 to 3 [24,25]. Therefore, a conservative systematic uncertainty of 30% is introduced in the present analysis.

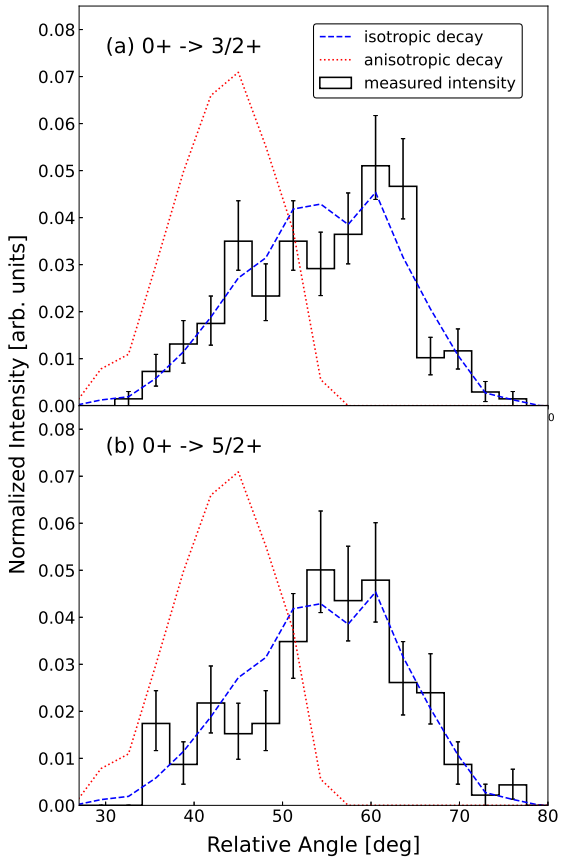

Fig. 7. The results of isotropic and anisotropic proton decay considerations for two transitions; from $J^\pi = 0^+$ (E_x = 7.218 MeV of ^{22}Mg) to (a) $J^\pi = 3/2^+$ (ground state of ^{21}Na) and (b) $J^\pi = 5/2^+$ (first excited state of ^{21}Na). The black solid lines represent the experimental distributions. The blue dashed lines and the red dotted lines are the results of the isotropic and anisotropic decay calculations, respectively. The error bars represent the statistical uncertainty of experimental distributions.

3 Discussion

The ^{21}Na(p, γ)^{22}Mg reaction rate can be expressed using the narrow-isolated resonance formalism [29]:

$$N_A < \sigma v > = \frac{1.5399 \cdot 10^{11}}{(\mu T_9)^{3/2}} \times \sum_i (\omega\gamma)_i e^{-11.605 E_i/T_9} \text{ cm}^3/\text{s/mol}, \quad (3)$$

where i is the resonance index, E_i and $(\omega\gamma)_i$ are the resonance energy and strength in units of MeV, respectively, μ is the reduced mass of projectile and target nucleus in amu, and T_9 is the temperature in units of GK.

For a given resonance, the resonance strength $\omega\gamma$ is defined as

$$\omega\gamma \equiv \frac{2J+1}{(2J_p+1)(2J_{21Na}+1)} \frac{\Gamma_p \Gamma_\gamma}{\Gamma}, \quad (4)$$

where J, J_p, and J_{21Na} are the spins of the resonance, proton, and ^{21}Na, respectively. Γ, Γ_p and Γ_γ are the total width and partial widths of the compound nucleus, ^{22}Mg.

Since the proton decay branching ratio can be described as $\frac{\Gamma_p}{\Gamma}$ [13,24], the measured branching ratio values, B_{p0} and B_{p1}, give constraints on $\frac{\Gamma_{p0}}{\Gamma}$ and $\frac{\Gamma_{p1}}{\Gamma}$. However, to obtain precise values for the branching ratios, more information related to other open channels is still needed. For instance, the ^{22}Mg states at E_x = 6.766 and 6.876 MeV are open for the p0 and p1 decay channels. Only the p0 decay channel was observed in the present work.

The ^{21}Na(p, γ)^{22}Mg reaction rate was calculated using the branching ratio values deduced from the present work. The resonance strength of

$$\omega\gamma_0 = \frac{2J+1}{(2J_p+1)(2J_{21Na}+1)}\frac{\Gamma_{p0}\Gamma_\gamma}{\Gamma} = \frac{2J+1}{(2J_p+1)(2J_{21Na}+1)}B_{p0}\Gamma_\gamma \quad (5)$$

was used for the calculation. Considering the Gamow window for X-ray bursts, two ^{22}Mg levels studied in the present work (E$_x$ = 6.766 and 6.876 MeV) were considered. The reaction Q-value of 5504.18 ± 0.34 keV was adopted from Ref. [30].

The gamma width value of the 6.876 MeV level was deduced from the mirror state (E$_x$ = 7.051 MeV in ^{22}Ne [14,17]), since no experimental data exists. Assuming that the reduced transition probability values B(ωL) are same for both states, the gamma width value of 4 ± 2 meV was obtained.

In the case of the 6.766 MeV state, the Γ_p value was measured twice in Ref. [9] and [16]. In Ref. [9], the reported values are Γ_{p0} = 93.9 ± 32.0 keV, Γ_{p1} = 11.1 ± 0.8 keV and $\Gamma_{p0} + \Gamma_{p1} \approx \Gamma_{total}$ = 105.0 ± 32.8 keV. In Ref. [16], only the $\Gamma_p = \Gamma_{p0}+\Gamma_{p1}$ value was reported as 64 ± 20 keV. Since the Γ_p values from the references are discrepant, the Γ_{p0} value, and subsequently the $\Gamma_{total} = \frac{\Gamma_{p0}}{B_{p0}}$, could not be constrained reliably. Furthermore, the corresponding mirror state is not well defined. For instance, Matic *et al.* suggested that the E$_x$ = 6.900 MeV level (J$^\pi$ = 0$^+$) in ^{22}Ne is the mirror state [14]. However, the spin value of the level from other studies show discrepancies with this suggestion: J$^\pi$ = (1$^+$, 2$^+$) [16], 3$^-$ [11,12], and 2$^-$ [9,17]. The mirror assignment of the 6.766 MeV level was not given in Ref. [17] Therefore, the gamma width of the level was assumed to be 1±1 eV in the present work as previously done in Ref. [31] for the ^{19}Ne level parameter estimations. The spin value is presumed to be 2$^-$ [9,17]. The resonance parameters used in the reaction rate calculation are summarized in Table 2. Except for the 6.766 and 6.876 MeV levels, the parameters were taken from Ref. [6].

Table 2. The resonance parameters used in the reaction rate calculation. The Q-value was taken from [30]. Parameters for the levels between E$_x$ = 5.711 and 6.608 MeV are taken from Ref. [6].

E$_x$ [MeV]	E$_r$ [keV]	J$^\pi$	$\omega\gamma$ [meV]
5.711	205.7±0.5	2$^+$	1.03±0.21
5.954	454±5	0$^+$	0.86±0.29
6.043	538±13	0$^+$	11.5±1.36
6.246	738.4±1.0		219±25
6.326	821.3±0.9	1+	556±77
6.608	1101.1±2.5	2+	368±62
6.766	1262±12[1]	2^{-}[2]	338±343[3]
6.876	1372±1[1]	1$^-$	1.22±0.89[3]

[1]Calculated with the corresponding excitation energies and the Q-value

[2]Taken from Ref. [9,17]

[3]Calculated with the gamma width and the branching ratio values deduced in the present work

The result of the reaction rate calculation is shown in the Fig. 8 as a red dashed line. The pink band in the

figure represents the upper and lower limits of the reaction rate. The reaction rate reported in Ref. [6] is also shown as a black solid line for comparison. The upper and lower limits of the previous rate is represented by a gray shaded area. At the astrophysical temperatures ($1 < T_9 < 2$), the new reaction rate is up to 2% higher than that of Ref. [6]. Notice that the present reaction rate calculated using the resonance strength expressed in Eq. 3 could be regarded as a lower limit, since only the p0 channel was considered. The most dominant uncertainty in the present rate originates from the uncertain gamma width for the 6.766 MeV level. Therefore, more precise measurements aiming to obtain the resonance parameters, especially the decay widths such as Γ_γ, and B_p are required in the future to obtain a better estimate of the ^{21}Na(p, γ)^{22}Mg reaction rate.

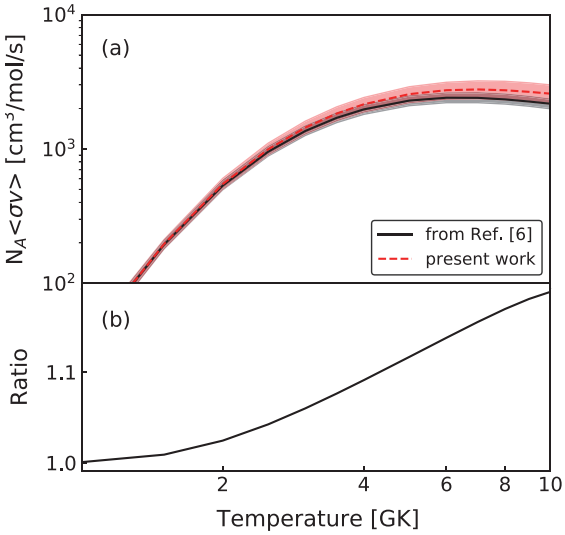

Fig. 8. The ^{21}Na(p, γ)^{22}Mg reaction rate calculation result. The present result is compared with that of Ref. [6] in (a). The pink and gray shading area represent the upper and lower limits of present rate and the reaction rate from Ref. [6], respectively. The ratio $N_A < \sigma v >_{present}/N_A < \sigma v >_{Iliadis}$ is shown in (b).

4 Conclusion

By investigating the decay protons from ^{22}Mg states populated through the previously reported ^{24}Mg(p, t)^{22}Mg transfer reaction study [15], the proton decay branching ratios of several ^{22}Mg levels (E_x = 6.766, 6.876, 7.218, 7.599, and 7.810 MeV) were obtained. By requiring coincidences between the reaction tritons and decay protons, the two-dimensional energy spectrum of E_p versus E_t was obtained in this follow up analysis. The events from the ^{24}Mg(p, t)^{22}Mg*(p)^{21}Na$_{g.s}$ channel and the ^{24}Mg(p, t)^{22}Mg*(p)^{21}Na* (E_x = 0.331 MeV) channel were identified. The triton energy spectra were constructed accordingly. From the triton energy spectrum, the energy levels of ^{22}Mg were identified. The yields of tritons and protons were obtained at each identified excited states. The yields of protons were corrected by considering the detection efficiency. The proton yields were then compared with that of the reaction tritons to obtain the proton branching ratios. The isotropic proton decay assumption was verified for the calculations. Using the branching ratio values for the 6.766 and 6.876 MeV levels obtained from the present work, the ^{21}Na(p, γ)^{22}Mg reaction rate at XRB temperatures was calculated. The result shows that the new rate is slightly higher than the previous values reported in Ref. [6].

This work was supported by the National Research Foundation of Korea (NRF) grants funded by the Korea government (MSIT) (Grants No. 2016R1A5A1013277, and No. 2020R1A2C1005981). Additionally, the research was supported in part by the National Nuclear Security Administration under the Stewardship Science Academic Alliances program through the U.S. DOE Cooperative Agreement No. DE-FG52-08NA28552 with Rutgers University and Oak Ridge Associated Universities. This work was also supported in part by the Office of Nuclear Physics, Office of Science of the U.S. DOE under Contract No. DE-FG02-96ER40955 with Tennessee Technological University, Contract No. DE-FG02-96ER40983 with the University of Tennessee, and Contract No. DE-AC-05-00OR22725 with Oak Ridge National Laboratory; by the National Science Foundation under Contract No. PHY-2011890 with the University of Notre Dame and Contract No. PHY-1812316 with Rutgers University.

References

1. J.L. Fisker, F.K. Thielemann, M. Wiescher, Astrophys. J. **608**(1), L61 (2004)
2. M. Wiescher, J. Görres, H. Schatz, J. Phys. G: Nucl. Part. Phys **25**(6), R133–R161 (1999).
3. H. Schatz, K. Rehm, Nucl. Phys. A **777**, 601–622 (2006).
4. J.L. Fisker, H. Schatz, F.K. Thielemann, Astrophys. J., Suppl. Ser. **174**(1), 261 (2008).
5. R.H. Cyburt *et al.*, Astrophys. J., Suppl. Ser. **189**(1), 240 (2010).
6. C. Iliadis, R. Longland, A. Champagne, A. Coc, R. Fitzgerald, Nucl. Phys. A **841**(1), 31 (2010).
7. T. Rauscher, Online code NON-SMOKER^{WEB},version 5.0w and higher. Https://nucastro.org/websmoker.html
8. J.M. D'Auria *et al.*, Phys. Rev. C **69**, 065803 (2004).
9. C. Ruiz *et al.*, Phys. Rev. C **71**, 025802 (2005).
10. R.A. Paddock, Phys. Rev. C **5**, 485 (1972).
11. A.A. Chen, R. Lewis, K.B. Swartz, D.W. Visser, P.D. Parker, Phys. Rev. C **63**, 065807 (2001).
12. J.A. Caggiano, W. Bradfield-Smith, J.P. Greene, R. Lewis, P.D. Parker, K.E. Rehm, D.W. Visser, Phys. Rev. C **66**, 015804 (2002).
13. B. Davids *et al.*, Phys. Rev. C **68**, 055805 (2003).
14. A. Matic *et al.*, Phys. Rev. C **80**, 055804 (2009).
15. K.Y. Chae *et al.*, Phys. Rev. C **79**, 055804 (2009).
16. J.J. He *et al.*, Phys. Rev. C **80**, 015801 (2009).
17. L.Y. Zhang *et al.*, Phys. Rev. C **89**, 015804 (2014).
18. P.D. Kunz, Http://spot.colorado.edu/ kunz/DWBA.html
19. J.R. Beene *et al.*, AIP Conference Proceedings **1336**(1), 576 (2011).
20. D.W. Bardayan *et al.*, Phys. Rev. C **63**, 065802 (2001).
21. B. Davids *et al.*, Phys. Rev. C **67**, 012801 (2003).
22. S. Utku *et al.*, Phys. Rev. C **57**, 2731 (1998).
23. M.S. Basunia, Nucl. Data Sheets **127**, 69 (2015).
24. K.A. Chipps *et al.*, Phys. Rev. C **82**, 045803 (2010).
25. K.A. Chipps *et al.*, Phys. Rev. C **86**, 014329 (2012).
26. K.A. Chipps *et al.*, Phys. Rev. C **95**, 044319 (2017).
27. M.J. Kim *et al.*, Phys. Rev. C **104**, 014323 (2021).
28. C.H. Kim *et al.*, Phys. Rev. C **105**, 025801 (2022).
29. C. Iliadis, *Nuclear Physics of Stars*, 2nd edn. (Wiley-VCH, Weinheim 2015) 183
30. M. Mukherjee *et al.*, Phys. Rev. Lett. **93**, 150801 (2004).
31. C.D. Nesaraja, N. Shu, D.W. Bardayan, J.C. Blackmon, Y.S. Chen, R.L. Kozub, M.S. Smith, Phys. Rev. C **75**, 055809 (2007).